

# On the application of differences in intrinsic fluctuations of Cherenkov light images for separation of showers.

V. V. Bugayov<sup>a,1</sup> A. V. Plyasheshnikov<sup>a</sup> V. V. Vassiliev<sup>b</sup>  
T. C. Weekes<sup>b</sup>

<sup>a</sup>*Department of Physics, Altai State University, Dimitrova 66, Barnaul, Russia, 656099*

<sup>b</sup>*Fred Lawrence Whipple Observatory, Harvard-Smithsonian CfA, P.O. Box 97, Amado, AZ 85645-0097*

---

## Abstract

The sensitivity of ground-based imaging atmospheric Cherenkov  $\gamma$ -ray observatories depends critically on the primary particle identification methods which are used to retain photon-initiated events and suppress the spurious background produced by cosmic rays. We suggest a new discrimination technique which utilizes differences in the fluctuations of the light intensity in the images of showers initiated by photons and those initiated by protons or heavier nuclei. The database of simulated events for the proposed VERITAS observatory has been used to evaluate the efficiency of the new technique. Analysis has been performed for both a single VERITAS imaging telescope, and a system of these telescopes. We demonstrate that a discrimination efficiency of  $\geq 1.5 - 2.0$  can be achieved in addition to traditional background rejection methods based on image shape parameters.

*Key words:* Gamma ray astronomy; Cosmic Ray Background

---

## 1 Introduction

Gamma-ray astronomy in the energy range above 100 GeV has made dramatic progress in the last decade due to rapid development of the atmospheric

---

<sup>1</sup> Corresponding author: bugaev@theory.dcn-asu.ru

Cherenkov technique at a number of ground-based  $\gamma$ -ray observatories. Detection of Cherenkov radiation from atmospheric cascades initiated by high energy particles has been considered as a potentially promising method for high energy  $\gamma$ -ray astronomy since the fifties [1] due to the large collecting area of the technique,  $\sim 5 \times 10^4 \text{ m}^2$ . Only recently, however, has it become possible to overcome the main factor limiting the sensitivities of ground-based observatories which utilize this method. This is the high rate of the cosmic ray (CR) background events. Introduction of the two techniques, imaging and stereoscopy, pioneered by the Whipple and HEGRA collaborations respectively [2,3], has made a drastic improvement in the suppression of the background, and has made possible the reliable detection and spectroscopy of several galactic and extragalactic sources [4–7]. Recent reviews of the development of high energy ground-based  $\gamma$ -ray astronomy can be found in [8,9].

Methods for the efficient discrimination of photon and hadron initiated events have been derived from the differences in the intrinsic properties of the Cherenkov radiation from purely electromagnetic and hadronic cascades. The most prominent of these is the substantially wider distribution of the arrival directions of photons in hadronic showers due to an additional angular scattering of the secondary products during hadronic interactions. This effect has been extensively studied in Monte-Carlo simulations of the cascade development in the atmosphere [18,17], and the rejection criteria for the cosmic ray background has been derived in the form of the so-called “shape cut” [10,11]. Increased angular resolution of ground-based  $\gamma$ -ray observatories together with this means of identification of the primary photon are the most important components of the recent discoveries and advances made in the highest energy  $\gamma$ -ray astronomy.

The confidence of discovery of a  $\gamma$ -ray source in the case of a background dominated data sample is defined as

$$R = \frac{N_{\text{on}} - N_{\text{off}}}{\sqrt{2N_{\text{off}}}}, \quad (1)$$

where  $N_{\text{on}}$  is the number of detected events produced by a hypothetic source for a given exposure, and  $N_{\text{off}}$  is the number of background events for the same observation time. This quantity reflects an excess of events due to the presence of a source measured in units of background standard deviation shown in the denominator for a Poisson distribution. It is generally accepted that the existence of a source is established if  $R \geq 5$ .

By application of the background rejection procedure one increases the confidence of the source discovery due to elimination of the signal fluctuations connected with the background. The efficiency of the discrimination technique used to identify primary photons and reject cosmic ray events is expressed

then as

$$\eta = \frac{\kappa_\gamma}{\sqrt{\kappa_p}}, \quad (2)$$

where  $\kappa_\gamma$  and  $\kappa_p$  are the probabilities of acceptance of photon and background events after the application of selection criteria. Thus the  $\eta$  factor is an enhancement of  $R$  indicating that  $\eta^2$  times less exposure is required for a source discovery when a new discrimination technique is applied. This is true in the case of background dominated regime, when  $N_{\text{on}} - N_{\text{off}} \leq N_{\text{off}}$ . On the contrary, in the statistics dominated regime ( $N_{\text{on}} - N_{\text{off}} \gg N_{\text{off}}$ ), background rejection procedures with  $\kappa_\gamma$  remarkably smaller than 1 should be avoided.

In this paper we explore a new discrimination technique that is characterized by efficiency  $\eta = 1.5 - 2$  in addition to the already existing methods of background suppression achieved by imposing shape and orientation cuts. This technique is based on the differences in intrinsic fluctuations of Cherenkov radiation produced in the pure electromagnetic and hadronic cascades. We adapt the maximum likelihood approach based on an analysis of the  $\chi^2$  functional to establish discrimination criteria to distinguish showers initiated by  $\gamma$ -rays from those initiated by CR nuclei. This idea was induced originally by the study of the mass composition of primary cosmic radiation [12] where similar methods were proved to be very successful.

## 2 The intrinsic fluctuations of the image

The imaging atmospheric Cherenkov telescope (IACT) consists of a set of mirrors on a single mount with a two-dimensional array of close-packed hexagonal photomultiplier tubes (pixels) in the focal plane. Therefore information about an event is recorded in the form of a two-dimensional image describing the distribution of the light intensity in the focal plane. Ultimately, the Cherenkov light image is a set of ADC counts corresponding to all pixels. But for simplicity we deal with the number of photoelectrons emitted from the pixels' photocathodes. Hence the Cherenkov light intensity in the focal plane is characterized by the continuous two dimensional distribution of photoelectron density,  $\rho(x, y)$ . Each point  $(x, y)$  on the focal plane corresponds to a certain arrival direction of photons relative to the pointing of the telescope mount. The total number of photoelectrons (pes) in the Cherenkov light image, *SIZE*, is given by

$$SIZE = \int \rho(x, y) \, dx \, dy.$$

In our further calculations we make frequent use of the normalized to unity distribution of photoelectrons

$$f(x, y) = SIZE^{-1} \rho(x, y), \quad (3)$$

which is equivalent to the probability density function (pdf). By translation and rotation of the reference frame it is always possible to choose a new coordinate system  $(x, y)$  in which the first moments of  $f(x, y)$  are equal to zero and the matrix of second moments is diagonalized. The diagonal elements

$$\int x^2 f(x, y) \, dx \, dy = LENGTH^2$$

$$\int y^2 f(x, y) \, dx \, dy = WIDTH^2,$$

which characterize the extent of the Cherenkov light distribution along the major and minor axes of the image, are often used as the image shape parameters.

Let us denote also the marginal distributions

$$f_L(x) = \int f(x, y) \, dy,$$

$$f_W(y) = \int f(x, y) \, dx,$$

where indices  $L$  and  $W$  correspond to the major and minor axes of the image respectively. We estimate  $f_L(x)$  and  $f_W(y)$  by the grid functions

$$N_{L,k} = \int_{x_k}^{x_{k+1}} f_L(x) \, dx, \quad x_{k+1} = x_k + \Delta x;$$

$$N_{W,k} = \int_{y_k}^{y_{k+1}} f_W(y) \, dy, \quad y_{k+1} = y_k + \Delta y;$$

defined at  $\{x_k, y_k; k = 1, \dots, K\}$ .

Suppose that we have two sets of shower images, initiated by photons and cosmic rays, for which the mean values,  $\bar{N}_{t,k}^{(\gamma)}$ ,  $\bar{N}_{t,k}^{(p)}$ , and variances,  $\sigma_{N_{t,k}^{(\gamma)}}^2$ ,  $\sigma_{N_{t,k}^{(p)}}^2$  of the grid functions are found for each  $k, t \in \{L, W\}$ . For each image we construct a pair of functionals  $\chi_t^2$

$$\chi_t^2 = \frac{1}{K} \sum_{k=1}^K \frac{(N_{t,k} - \bar{N}_{t,k}^{(\gamma)})^2}{\sigma_{N_{t,k}}^{(\gamma)^2}} \quad (4)$$

so that the mean values of  $\chi_t^2$  for  $\gamma$ -showers and background events are equal to:

$$\overline{\chi_t^{2(\gamma)}} = 1; \quad \overline{\chi_t^{2(p)}} = \frac{1}{K} \sum_{k=1}^K \left[ \frac{\sigma_{N_{t,k}}^{(p)}}{\sigma_{N_{t,k}}^{(\gamma)}} \right]^2 + \frac{1}{K} \sum_{k=1}^K \left[ \frac{\bar{N}_{t,k}^{(\gamma)} - \bar{N}_{t,k}^{(p)}}{\sigma_{N_{t,k}}^{(\gamma)}} \right]^2. \quad (5)$$

The  $\overline{\chi_t^{2(p)}}$  consists of two terms. The first term reflects the differences in the fluctuations of the light intensity of images initiated by  $\gamma$ -rays and those initiated by CR particles. The second one characterizes the differences between the average shapes of distributions of the photoelectron density in the images of the two data sets.

Strickly speaking, two different effects influence the value of the "fluctuation" term of  $\chi_t^{2(p)}$ . The first of them is connected with random variations of the angular size of the image described, for example, by WIDTH and LENGTH parameters. The second effect is the irregularity of the light distribution inside the image itself. We say in this case about the intrinsic fluctuations. Even in the case of  $\gamma$ -ray and proton induced images having the same angular size the first of them has a more smooth and regular structure and, therefore, a smaller value of intrinsic fluctuations. Large fluctuations in the number of secondary particles created during the hadron multi-particle production is the main reason of difference in intrinsic fluctuations of  $\gamma$ - and  $p$ -induced images.

In this work we attempt to make use of the contribution to  $\overline{\chi_t^{2(p)}}$  from the first ("fluctuation") term because we expect that the second term (as well as the fluctuations connected with variations of the angular size of the image) is rather small for images which passed the image shape selection criteria.

Keeping in mind the argumentation presented above, one can hope to use selection criteria of the form

$$\chi_L^2 < \tilde{\chi}_L^2, \quad \chi_W^2 < \tilde{\chi}_W^2 \quad (6)$$

to reject CR-induced events and retain genuine photon-initiated showers. For a single telescope, two constants  $\tilde{\chi}_L^2$  and  $\tilde{\chi}_W^2$  should be optimized to maximize the signal to noise ratio (see formula (1)). For a system of telescopes a set of similar criteria can be utilized

$$\chi_{L,i}^2 < \tilde{\chi}_L^2, \quad \chi_{W,i}^2 < \tilde{\chi}_W^2, \quad i = 1, \dots, N_{\text{trig}}, \quad (7)$$

in which condition (6) is satisfied simultaneously for all triggering telescopes. We consider a slightly more relaxed background rejection criterion

$$\frac{1}{N_{\text{trig}}} \sum_{i=1}^{N_{\text{trig}}} \chi_{L,i}^2 < \tilde{\chi}_L^2, \quad \frac{1}{N_{\text{trig}}} \sum_{i=1}^{N_{\text{trig}}} \chi_{W,i}^2 < \tilde{\chi}_W^2 \quad (8)$$

which seems to retain more photon-initiated events and produce a higher efficiency factor (2). In the case of a single telescope, both criteria (6) and (8) are identical.

The success of a selection criterion depends dramatically on how the data sets of photons and CR nuclei have been selected. In order to increase the selection efficiency one should consider the smaller regions of the primary photon parameter phase space and formulate selection criteria for each of them. We expect that the shower parameters which affect background rejection most strongly are the primary energy,  $E$  and the impact parameter,  $r$  (the shortest distance between the telescope and the cascade core). In order to make the  $\chi^{2(\gamma)}$  distribution narrower and thus improve the discrimination ability of the method, we will evaluate the dependence of the grid functions of photoelectron density on these parameters

$$N_{t,k} = N_{t,k}(E, r), \quad \bar{N}_{t,k}^{(\gamma)} = \bar{N}_{t,k}^{(\gamma)}(E, r), \quad \sigma_{N_{t,k}^{(\gamma)}} = \sigma_{N_{t,k}^{(\gamma)}}(E, r). \quad (9)$$

We would like to note that the  $\chi^2$ -based method has been used in the past to deduce parameters of the primary particle [13,14]. In our work, however, we do not explicitly assume that the fluctuations in the images of  $\gamma$ -rays are of a Poissonian nature.

### 3 Data sets of shower images

To investigate the discrimination efficiency of the method we have simulated two data bases of photon and proton initiated showers. This task has been accomplished by utilizing ALTAI computation code [15] with input data summarized in Table 1. The geometrical layout of the VERITAS array of telescopes is shown in Fig. 1. Although, both proton and photon induced cascades were simulated as vertical showers, images of cosmic rays were also sampled isotropically on the focal planes of the telescopes near the vertical direction. 44,000 and 92,000 showers were simulated for photons and protons respectively. The position of the shower core was distributed uniformly inside a circle with radius of 300 m centered on the central telescope of the VERITAS array. A

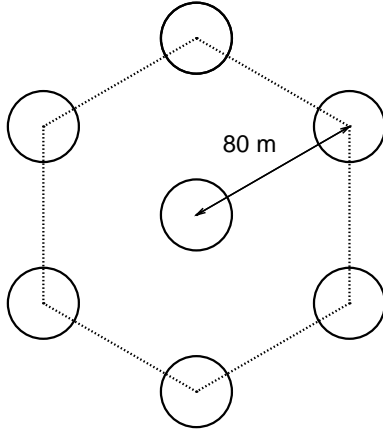


Fig. 1. Layout of VERITAS telescopes.

power law differential energy spectra of primary particles was assumed with exponent  $-2.6$  for photons and  $-2.75$  for protons. Photons were sampled from the energy interval  $0.05 - 10$  TeV and protons were distributed between  $0.1 - 20$  TeV.

The contribution of the night sky background was taken to be one photoelectron per pixel. We applied a rather severe cleaning algorithm which insured that only bright images with light intensity well above this background were included in our analysis. Shower images were processed in two stages. First, all pixels with less than five photoelectrons were excluded from further consideration. Then, only pixels which contained more than nine photoelectrons or which had a neighbor pixel with a nonzero content were assumed to be image pixels. In addition, only images with *SIZE* greater than 100 photoelectrons were accepted for the analysis. The telescope was considered to be triggered when at least two pixels from an internal zone of the multichannel camera (331 inner pixels) detected more than 20 photoelectrons. Finally, to ensure the high quality of images, only telescopes with maximal light intensity of the image in the internal zone were accepted.

Table 1

Basic parameters of VERITAS telescopes

Number of telescopes	7
Altitude above the sea level, [m]	1500
Area of the mirror, [m <sup>2</sup> ]	78
Number of pixels	547
Pixel size, [degree]	0.15
Field of view, [degree]	$\simeq 4.0$

## 4 Determination of the impact parameter

The efficiency factor,  $\eta$ , of the discrimination technique increases if the dependence of the image photoelectron density on the energy and the impact parameter of a shower is accounted for (formula(9)). Therefore, it is necessary to have some method of determining these quantities. In this work we have investigated three possibilities for estimating impact parameter of the primary particle:

- VERITAS operates as a system of telescopes. The impact parameter is determined by a simple geometrical event reconstruction method (see, e.g., [11]).
- VERITAS operates in a single telescope mode.
  - The impact parameter is determined on the basis of the *DIST* (distance) parameter of the image.
  - The impact parameter is determined by means of the *ELLIPT* (ellipticity) parameter of the image.

Stereoscopic observation of an event by at least two telescopes allows unambiguous geometrical reconstruction of the shower core location in space. If the number of telescopes which detected an event is larger than two it is possible to increase the accuracy in determining this parameter. In this work we use as an estimate of the shower core location, a weighted average of the core coordinates derived from the data of each pair of triggered telescopes [13].

For a single telescope, determination of the impact parameter utilizes its correlation with such characteristics of the image, as *ELLIPT* or *DIST* [16] defined as

$$ELLIPT = \frac{LENGTH}{WIDTH} - 1, \quad DIST = \sqrt{x_c^2 + y_c^2}, \quad (10)$$

where  $x_c$  and  $y_c$  are coordinates of the image centre of gravity in the reference frame with an origin at the source location. Unlike the *DIST* parameter, *ELLIPT* provides an opportunity for determining the impact parameter not only for a point-like, but also for an extended  $\gamma$ -ray sources when the arrival direction of a photon is not known. To derive our estimate of impact parameter in the case of a single telescope observations, we tabulated mean values of *ELLIPT* and *DIST* for a set of values of impact parameter and image *SIZE*. The required estimate of  $r$  was then calculated by backward interpolation. In fig. 2 we show the dependence of mean *DIST* on the impact parameter for several intervals of *SIZE*. Larger values of *SIZE* correspond to curves with larger values of *DIST*.

In fig.3 and tab.2 we show the accuracy of determination of the impact parameter by three different methods.



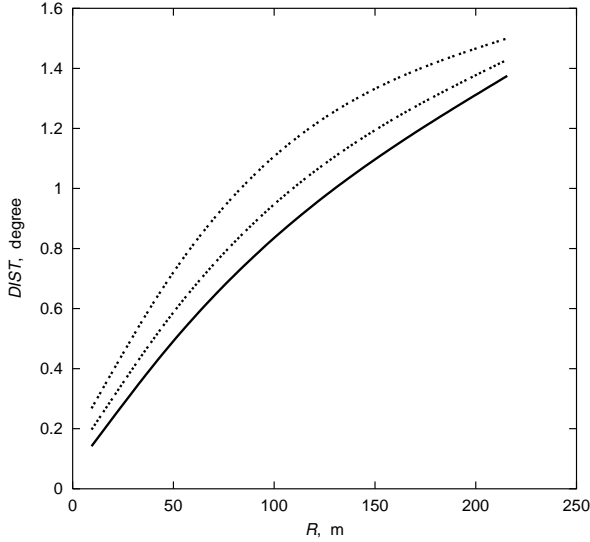


Fig. 2. Dependence of the  $DIST$  parameter on the impact parameter for  $\gamma$ -showers. The curves are calculated for  $SIZE$  intervals with the centres at 220 (bottom curve), 840, 3200 pes. (top curve) respectively.

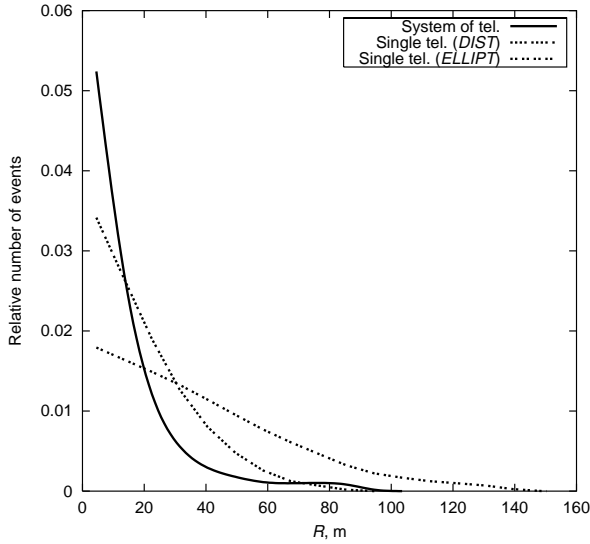


Fig. 3. The probability distribution for the error of determining the  $\gamma$ -shower impact parameter. The  $SIZE$  of the images is larger than 150 pes.

The accuracy of determining the impact parameter depends strongly on the lower bound of the  $SIZE$  of images included in the analysis. The smaller the  $SIZE$  of the shower image, the stronger the effects of fluctuations in image photoelectron density, and the stronger the influence of the night sky background. A large difference between the errors of impact parameter determination for photons and protons in the case of a system of telescopes is due to the inherent differences in the electron density distribution between the images of showers initiated by these primaries. While the distribution of Cherenkov light is smooth and compact for  $\gamma$ -rays, for protons it is fuzzy and

more extended. As a result the proton induced images (and their basic parameters determining the reconstructed value of the shower impact parameter) are more significantly distorted in the process of the cleaning procedure aimed at the elimination of the night sky background and consisting in an exclusion from consideration of pixels with low magnitudes.

In the case of the photon primary the method of impact parameter determination based on the *DIST* parameter is substantially more accurate than the one where the ellipticity is in use. Perhaps, this can be explained by the larger fluctuations of the *ELLIPT* parameter, or in other words by weaker correlation of *ELLIPT* with shower core location. The "ELLIPT" based method indicates a substantially smaller error on the impact parameter determination for  $\gamma$ -induced air showers relative to proton initiated ones, which can also be explained by the larger fluctuations of the light intensity in CR-induced images. For isotropically distributed cosmic rays one should not expect any correlation between the impact parameter of the showers and the *DIST* value. The error on the determination of the shower core location of 53 m, found in this case, is finite because of the limited telescope field of view and the high directionality of the distribution of Cherenkov photons from atmospheric cascades.

## 5 Event selection based on the shape parameters

To estimate the discrimination efficiency of this new technique, we applied a preliminary event selection on the basis of the shape parameters (*WIDTH* and *LENGTH*) thereby excluding any possible correlation between the traditional and proposed event classification methods. In this work we adapted a selection criterion in the form

$$\frac{WIDTH}{\bar{W}^{(\gamma)}(SIZE, r)} \leq \tilde{W}_{sc}, \quad i = 1, \dots, N_{\text{trig}} \quad (11)$$

where  $\bar{W}^{(\gamma)}(SIZE, r)$  is the mean value of *WIDTH* for  $\gamma$ -showers detected with a given image *SIZE* and estimated impact parameter,  $r$ , (fig. 4). Ap-

Table 2

The value of the impact parameter determination error [m]. 50% of showers have an error smaller than the value presented in the table. The *SIZE* of the images is larger than 150 pes.

	$\gamma$	$p$
System of telescopes	5	32
Single telescope ( <i>DIST</i> )	11	53
Single telescope ( <i>ELLIPT</i> )	27	68

plication of this criterion, commonly known as the scaled width method [11], turns out to be particularly effective as it accounts for the changes of image *WIDTH* caused by the differences in primary photon energy and the possible variations in the shower core location. We excluded *LENGTH* as a discrimi-

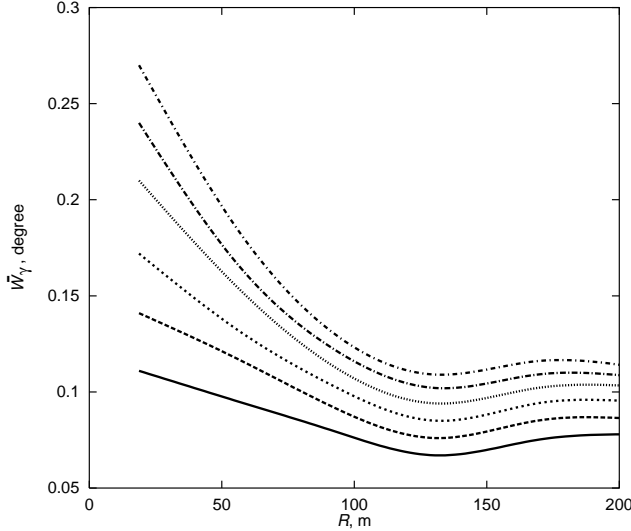


Fig. 4.  $\bar{W}^\gamma = f(\text{SIZE}, r)$ . The curves are calculated for *SIZE* intervals with the centres at 220 (bottom curve), 430, 840, 1600, 3200, 6200 pes (top curve), respectively

nation parameter while using  $W_{\text{sc}}$ ; two-dimensional discrimination on the basis of *LENGTH* and *WIDTH* yields only negligible increase in  $\eta$  [11].

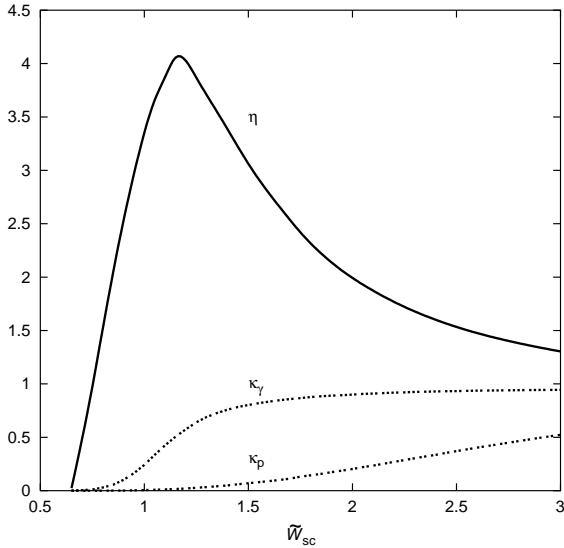


Fig. 5. Dependence of background discrimination efficiency  $\eta$ , true classification probability ( $\kappa_\gamma$ ) of  $\gamma$ -rays, and false classification probability ( $\kappa_p$ ) of protons as functions of the  $W_{\text{sc}}$  cut. In this example, VERITAS operates as an array of telescopes.

In fig. 5 the dependence of background discrimination efficiency on  $\tilde{W}_{\text{sc}}$  cut

(11) is shown. The dependence of  $\eta$  on the true classification probability of  $\gamma$ -rays is shown, for different event reconstruction methods, in fig. 6.

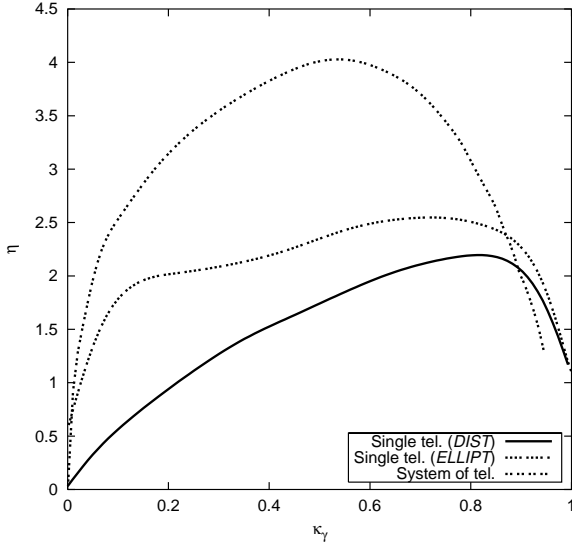


Fig. 6. Dependence of the background discrimination efficiency  $\eta$  on the true classification probability  $\kappa_\gamma$  of photons.

## 6 Optimization of the discrimination technique

Fig. 7 depicts two histograms: the ratio of the mean photoelectron density along the major axis ( $t = L$ ) for images initiated by photons and protons (1), and the ratio of their standard deviations (2). The *SIZE* parameter was limited within interval from 100 to 200 photoelectrons, and the actual shower impact parameter was restricted to the 50 – 75 m interval. The values of these intervals were chosen as small as the statistics allows in order to reduce the fluctuations connected with random variations of the primary energy and of the impact parameter.

It can be seen that for the given conditions, the contribution to the  $\chi^2$  functional (Eq. 5) from the first, “fluctuation”, term exceeds the second, “mean difference”, term by almost a factor of ten. This confirms our assumption about the potential of the Cherenkov light intensity fluctuations for discriminating proton and  $\gamma$ -induced images.

The bin sizes,  $\Delta x = 0.2^\circ$  and  $\Delta y = 0.06^\circ$ , used to construct the grid photoelectron density functions, were optimized to achieve the highest discrimination efficiencies. They are chosen as a balance between the necessity to resolve features in the shower images on the scales smaller than *LENGTH* and *WIDTH* and, at the same time, not to make fluctuations in the bins dominated by Poisson statistics. In addition, a special analysis has shown that the  $\chi^2$ -technique

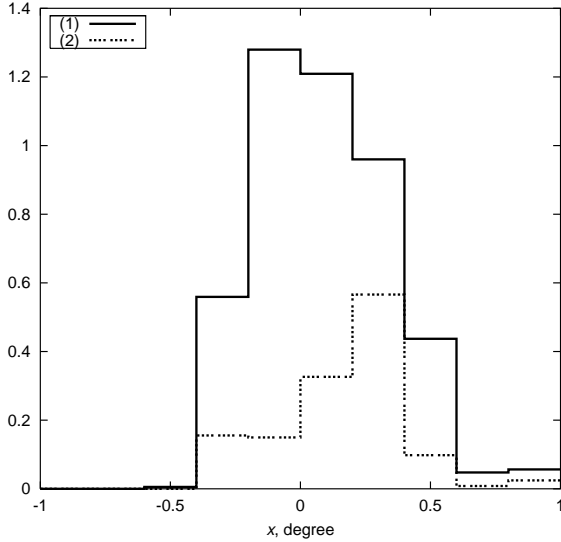


Fig. 7.  $\bar{N}_{L,k}^{(\gamma)}/\bar{N}_{L,k}^{(p)}$  (1) and  $\sigma_{N_{L,k}^{(\gamma)}}/\sigma_{N_{L,k}^{(p)}}$  (2) for events surviving the scaled width cut ( $W_{sc} = 1.4$ , *DIST*-approach). A single VERITAS telescope is considered. Bin size  $\Delta x = 0.2^\circ$ .

exhibits no essential sensitivity to the bin size if the value of this size does not exceed considerably the pixel size ( $0.15^\circ$ ) of the VERITAS telescopes.

The comparison of the probability distributions  $\chi_L^2$  and  $\chi_W^2$  for  $\gamma$  and  $p$ -induced events, for a single telescope, is shown in fig. 8. Tab. 3 summarizes the photon

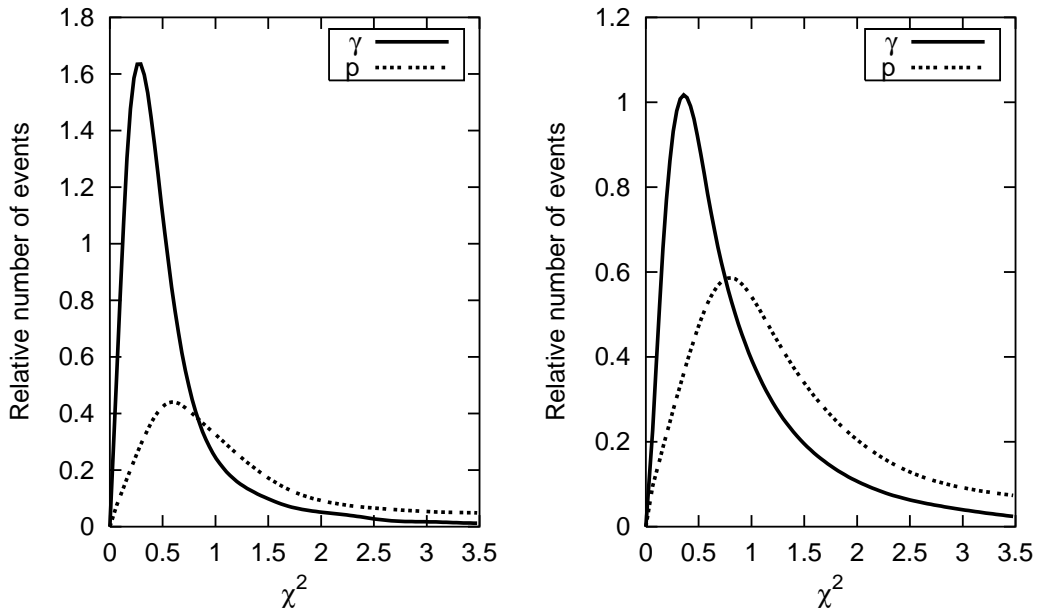


Fig. 8. Probability distributions for  $\chi_L^2$  (on the left) and  $\chi_W^2$  (on the right) for a single VERITAS telescope after  $W_{sc} = 1.3$  cut is applied. Determination of the impact parameter is based on *DIST* parameter.

selection efficiency after application of the scaled width cut,  $(\kappa_{\gamma W}, \eta_W)$ , and

after discrimination of background using the  $\chi_L^2$  and  $\chi_W^2$  parameters (eqn. 8), ( $\kappa_{\gamma\chi}, \eta_\chi$ ). These calculations were performed for the full VERITAS array. The first column indicates the value of  $\tilde{W}_{sc}$  cut. The total discrimination effect is denoted as ( $\kappa_{\gamma\text{tot}}, \eta_{\text{tot}}$ ).  $\kappa_{\gamma\chi}$  corresponds to the value of  $\chi_L^2$  and  $\chi_W^2$  cuts at which discrimination efficiency factor,  $\eta$ , is maximal provided that  $\kappa_{\gamma\chi} \geq 0.7$ .

Table 3

Summary of the background rejection efficiency for VERITAS.

$\tilde{W}_{sc}$	$\kappa_{\gamma W}$	$\eta_W$	$\kappa_{\gamma\chi}$	$\eta_\chi$	$\kappa_{\gamma\text{tot}}$	$\eta_{\text{tot}}$
1.15	0.52	4.11	0.81	1.41	0.42	5.80
1.20	0.60	4.08	0.74	1.43	0.44	5.83
1.25	0.67	3.90	0.79	1.58	0.53	6.16
1.3	0.72	3.87	0.82	1.66	0.59	6.42
1.4	0.79	3.55	0.70	1.84	0.55	6.53

It is evident from the table that the largest value of the total efficiency factor,  $\eta_{\text{tot}}$ , is achieved for  $\tilde{W}_{sc}$  larger than the value which provides maximum discrimination power of photon selection based solely on the scaled width cut. This is also correct for event reconstruction using a single telescope. Selection criterion utilizing only the  $\chi_L^2$  cut demonstrates a discrimination efficiency factor  $\simeq 80-90\%$  of the one obtained with the use of both  $\chi^2$  cuts. An increase of  $\tilde{W}_{sc}$  provides a moderate growth of photon discrimination efficiency when  $\chi_W^2$  is sequentially applied, while the effect of a  $\chi_L^2$  selection depends very weakly on the scaled width cut.

The plots of discrimination efficiency of  $\chi^2$  technique as a function of true photon classification probability,  $\kappa_\gamma$ , are shown in fig. 9 for various VERITAS event reconstruction methods. The scaled width cut was optimized to provide maximal total discrimination efficiency when  $\kappa_\gamma$  is fixed. Curves (1) and (2) in this figure compare the factor  $\eta$  for a  $\chi^2$  cut in the form given in (8) and (6) when the latter is applied to each VERITAS telescope in the event trigger. It can be seen that the discrimination efficiency of photon selection is higher for the case which uses the mean value of  $\chi^2$ .

In tab. 4 we present the true photon classification probability and discrimination efficiency of the  $\chi^2$  technique when various lower bounds on image *SIZE* are included in the analysis. The dependence of these quantities on the lower limit of the estimated energy of the primary particle is shown in the tab. 5. For both tables we tuned the scaled width cut to optimize the total efficiency factor. Primary energy was estimated by backward interpolation with respect to image *SIZE* and estimated impact parameter,  $r$ , using simulated data base of photon induced showers.

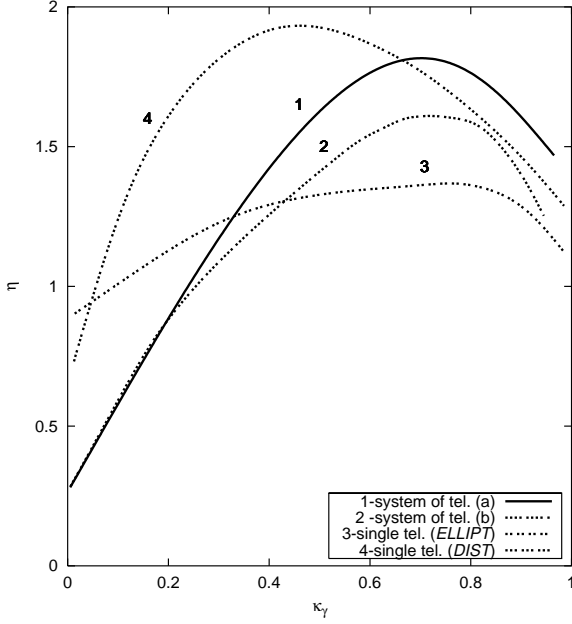


Fig. 9. Dependence of  $\chi^2$  selection efficiency  $\eta(\kappa_\gamma)$  for different event reconstruction methods. For array of telescopes, curve (a) corresponds to  $\chi^2$  selection criterion (8), and curve (b) is obtained for criterion (6) applied to each telescope participating in the VERITAS trigger.

Table 4

Discrimination efficiency of  $\chi^2$  photon selection technique ( $\tilde{W}_{sc}$  cut is tuned to maximize  $\eta_{tot}$ ). Different image *SIZE* lower bound for analyzed events is shown.

	System				Single( <i>DIST</i> )				Single( <i>ELLIPT</i> )			
$S$	100	150	200	300	100	150	200	300	100	150	200	300
$\kappa_\gamma$	0.75	0.70	0.71	0.71	0.73	0.70	0.73	0.70	0.79	0.71	0.70	0.70
$\eta_{\chi^2}$	1.50	1.84	1.94	2.14	1.43	1.81	2.34	4.11	1.22	1.37	1.56	1.95

Table 5

Discrimination efficiency of  $\chi^2$  photon selection technique as a function of lower bound on event estimated energy to be included into the analysis.

	System				Single ( <i>DIST</i> )				Single ( <i>ELLIPT</i> )			
$E_{est.}$ , [TeV]	0.2	0.3	0.5	1	0.2	0.3	0.5	1	0.2	0.3	0.5	1
$\kappa_\gamma$	0.72	0.73	0.70	0.71	0.70	0.70	0.71	0.70	0.72	0.71	0.71	0.70
$\eta_{\chi^2}$	1.91	2.00	2.19	3.33	1.62	1.97	2.31	3.92	1.52	1.65	1.76	2.47

## 7 Conclusion

In this work we have examined the feasibility of improving photon selection using differences in the fluctuations of the Cherenkov light distribution between the images of  $\gamma$  and  $p$ -initiated showers. Three different event reconstruction

methods which are likely be utilized in the next generation of ground-based  $\gamma$ -ray observatories, such as VERITAS, have been studied. Two of them are applicable to observations with a single telescope and one uses the stereoscopic capability of VERITAS array.

Optimization of our technique indicates that the proposed method provides an additional increase of the total discrimination efficiency by a factor  $\geq 1.5 - 2.0$  retaining the survival probability of  $\gamma$ -ray initiated events at the level larger than 0.7. That is true for both the telescope array and the single telescope (with estimation of impact parameter by the *DIST*-based method). The achievable value of the total discrimination efficiency is equal to 6.5 and 3.6 respectively. When a single telescope event is reconstructed utilizing the *ELLIPT* parameter, our approach provides an additional discrimination efficiency factor  $\geq 1.4$ . This is particularly important for a detection of extended sources or sources whose position has not been accurately identified . The discrimination efficiency of the proposed method increases rapidly with the energy of the primary photon.

## Acknowledgements

A.V. Plyasheshnikov thanks the Harvard-Smithsonian Center for Astrophysics for the opportunity to visit the Whipple Observatory. We acknowledge the help of Deirdre Horan and Stephen Fegan in preparation of the manuscript. This work was partially supported by the US Department of Energy.

## References

- [1] Galbraith, W. & Jelley, J.V., 1953, *Nature*, 171, 349
- [2] Reynolds, P.T., et al. 1993, *ApJ*, 404, 206
- [3] Aharonian, F.A., et al. 1993, *Workshop Towards a Major Atmospheric Cherenkov Detector*, 81
- [4] Weekes, T.C., et al. 1989, *ApJ*, 342, 379
- [5] Punch, M., et al. 1992, *Nature*, 358, 477
- [6] Quinn, J., et al. 1996, *ApJ*, 456, L83
- [7] Aharonian, F. A., et al. 1999, *A&A*, 349, 11A
- [8] Ong, R.A., 1998, *Phys. Rep.*, 305, 93
- [9] Catanese, M. & Weekes, T.C., 1999, *PASP*, 111, 1193



- [10] Fegan D.J., 1993, Workshop Towards a Major Atmospheric Cherenkov Detector
- [11] Aharonian, F.A., et al. 1997, Astroparticle Physics 6, 343
- [12] Plyasheshnikov, A.V., et al. 1998, J. Phys. G.: Nucl. Part. Phys., 24, 653
- [13] Ulrich, M., et al. 1998, J. Phys. G: Nucl. Part. Phys., 24, 883
- [14] Le Bohec, S., Degrange, B., et. al. 1998, astro-ph/9804133
- [15] A.K. Konopelko, A.V. Plyasheshnikov, Nucl. Instr. Meth. A 450(2000) 419-429.
- [16] Plyasheshnikov, A.V. & Konopelko, A.K., 1989, Proceedings of International Workshop on VHE  $\gamma$ -ray astronomy, (Crimea), 120
- [17] M. Hillas, Proceedings of 19th ICRC La Jolla, 5(1985) 445-449.
- [18] F. Aharonian et al. NIM A302 (1991) pp. 522-528.